Vector analysis of stimulated Brillouin scattering amplification in standard single-mode fibers

Avi Zadok[1, 2, *], Elad Zilka[1], Avishay Eyal[1], Luc Thévenaz[3], and Moshe Tur[1]

[1]*School of Electrical Engineering, Faculty of Engineering, Tel-Aviv University, Tel-Aviv 69978, Israel*
[2]*Currently with the Department of Applied Physics, MC 128-95, California Institute of Technology, Pasadena, CA 91125, USA*
[3]*Ecole Polytechnique Fédérale de Lausanne, Institute of Electrical Engineering, STI-GR-SCI Station 11, 1015 Lausanne, Switzerland*
[*]*Corresponding author: avizadok@caltech.edu*

Abstract: The polarization properties of stimulated Brillouin scattering (SBS) amplification or attenuation in standard single-mode fibers are examined through vectorial analysis, simulation and experiment. Vector propagation equations for the signal wave, incorporating SBS and birefringence, are derived and analyzed in both the Jones and Stokes spaces. The analysis shows that in the undepleted pump regime, the fiber may be regarded as a polarization-dependent gain (or loss) medium, having two orthogonal input SOPs, and corresponding two orthogonal output SOPs, for the signal, which, respectively, provide the signal with maximum and minimum SBS amplification (or attenuation). Under high Brillouin gain conditions and excluding zero-probability cases, the output SOP of arbitrarily polarized input signals, would tend to converge towards that of maximum SBS gain. In the case of high SBS attenuation the output SOP of an arbitrarily polarized signal would approach the output SOP corresponding to minimum attenuation. It is found that for a wide range of practical pump powers ($\leq 100\,\mathrm{mW}$) and for sufficiently long fibers with typical SBS and birefringence parameters, the signal aligned for maximum SBS interaction will enter/emerge from the fiber with its electric field closely tracing the same ellipse in space as that of the pump at the corresponding side of the fiber, albeit with the opposite sense of rotation. The analytic predictions are experimentally demonstrated for both Stokes (amplification) and anti-Stokes (attenuation) signals.

OCIS codes: (290.5900) Scattering, Stimulated Brillouin; (120.5410) Polarimetry.

References and links

1. T. Horiguchi, T. Kurashima, and M. Tateda, "A technique to measure distributed strain in optical fibers," IEEE Photon. Technol. Lett. **2**, 352-354, (1990).
2. M. Nikles, L. Thévenaz, and P. Robert, "Brillouin gain spectrum characterization in single-mode optical fibers," J. Lightwave Technol. **15**, 1842-1851, (1997).
3. X. Bao, D. J. Webb, and D. A. Jackson, "32-km distributed temperature sensor using Brillouin loss in optical fiber," Opt. Lett. **18**, 1561-1563, (1993).
4. J. C. Yong, L. Thévenaz, and B. Y. Kim, "Brillouin fiber laser pumped by a DFB laser diode," J. Lightwave Technol. **12**, 546-554, (2003).
5. A. Loayssa, D. Benito, and M. J. Grade, "Optical carrier-suppression technique with a Brillouin-erbium fiber laser," Opt. Lett. **25**, 197-199, (2000).
6. Y. Shen, X. Zhang, and K. Chen, "Optical single side-band modulation of 11 GHz RoF system using stimulated Brillouin scattering," IEEE Photon. Technol. Lett. **17**, 1277-1279, (2005).
7. A. Zadok, A. Eyal, and M. Tur, "GHz-wide optically reconfigurable filters using stimulated Brillouin scattering," J. Lightwave Technol. **25**, 2168-2174, (2007).
8. A. Loayssa, and F. J. Lahoz, "Broadband RF photonic phase shifter based on stimulated Brillouin scattering and single side-band modulation," IEEE Photon. Technol. Lett. **18**, 208-210, (2006).
9. A. Loayssa, J. Capmany, M. Sagues, and J. Mora, "Demonstration of incoherent microwave photonic filters with all-optical complex coefficients," IEEE Photon. Technol. Lett. **18**, 1744-1746, (2006).

#102564 - $15.00 USD Received 9 Oct 2008; revised 18 Nov 2008; accepted 12 Dec 2008; published 16 Dec 2008

10. Z. Zhu, D. J. Gauthier, and R. W. Boyd, "Stored light in an optical fiber via Stimulated Brillouin Scattering," Science **318**, 1748-1750, (2007).
11. M. González-Herráez, K.-Y. Song, and L. Thévenaz, "Optically controlled slow and fast light in optical fibers using stimulated Brillouin scattering," Appl. Phys. Lett. **87**, 081113, (2005).
12. M. D. Stenner, M. A. Neifeld, Z. Zhu, A. M. C. Dawes, and D. J. Gauthier, "Distortion management in slow-light pulse delay," Opt. Express **13**, 9995-10002, (2005).
13. Z. Zhu, A. M. C. Dawes, D. J. Gauthier, L. Zhang, and A. E. Willner, "Broadband SBS slow light in an optical fiber," J. Lightwave Technol. **25**, 201-206, (2007).
14. M. González-Herráez, K.-Y. Song, and L. Thévenaz, "Arbitrary-bandwidth Brillouin slow light in optical fibers," Opt. Express **14**, 1395-1400, (2006).
15. K. Y. Song, M. Gonzalez Herraez, and L. Thévenaz, "Observation of pulse delay and advancement in optical fibers using stimulated Brillouin scattering," Opt. Express **13**, 82-88, (2005).
16. A. Zadok, A. Eyal, and M. Tur, "Extended delay of broadband signals in stimulated Brillouin scattering slow light using synthesized pump chirp," Opt. Express **14**, 8498-8505, (2006).
17. R. W. Boyd, *Nonlinear optics*, (San Diego, CA: Academic Press, 2003) chapter 9, 409-427.
18. A. Yariv, *Optoelectronics*, (Orlando FL: Saunders College Publishing, 4th Edition, 1991), chapter 19, 670-678.
19. Z. Zhu, D. J. Gauthier, Y. Okawachi, J. E. Sharping, A. L. Gaeta, R. W. Boyd, and A. E. Willner, "Numerical study of all-optical slow-light delays via stimulated Brillouin scattering in an optical fiber," J. Opt. Soc. Am. B **22**, 2378-2384, (2005).
20. T. Horiguchi, M. Tateda, M. Shibata, and Y. Azuma, "Brillouin gain variation due to a polarization-state change of the pump or Stokes field in standard single mode fibers," Opt. Lett. **14**, 329-331, (1989).
21. M. O. van Deventer, and A. J. Boot, "Polarization properties of stimulated Brillouin scattering in single mode fibers," J. Lightwave Technol. **12**, 585-590, (1994).
22. In [21], the pump and probe SOPs are defined in two different reference frames, corresponding to opposite directions of propagation. In this work, as well as in most of the literature on polarization [23,24], a single reference frame is used. Therefore, we defer the mathematical description of the conditions for maximum/minimum SBS gain to Section 2.
23. R. C. Jones, "A new calculus for the treatment of optical system," J. Opt. Soc. Am. **37**, 107-110, (1947).
24. E. Collett, Ed., *Polarized light fundamentals and applications.* (New York: Marcel Dekker, 1993).
25. L. Thévenaz, A. Zadok, A. Eyal, and M. Tur, "All-optical polarization control through Brillouin amplification," paper OML7 in *OFC/NFOEC 2008*, San Diego, Ca, (2008).
26. J. P. Gordon and H. Kogelnik, "PMD fundamentals: polarization mode dispersion in optical fibers", P. Natl. Acad. Sci. USA **97**, 4541-4550, (2000).
27. R. H. Stolen, "Polarization effects in fiber Raman and Brillouin lasers," IEEE J. of Quantum Electron. **15**, 1157-1160, (1979).
28. F. Corsi, A. Galtarossa, and L. Palmieri, "Analytical treatment of polarization mode dispersion in single mode fibers by means of the backscattered signal," J. Opt. Soc. Am. A **16**, 574-583, (1999).
29. M. Brodsky, N. J. Frigo, ad M. Tur, "Polarization mode dispersion," chapter 17 in *Optical Fiber Telecommunications V-A*, Ed. I. P. Kaminow, T. Li and A. E. Willner, (Academic Press, 2008).
30. A. Loayssa, D. Benito, and M. J. Grade, "High resolution measurement of stimulated Brillouin scattering spectra in single-mode fibers," IEE Proc. Optoelectron. **148**, 143-148, (2001).
31. A. Eyal, D. Kuperman, O. Dimenstein, and M. Tur, "Polarization dependence of the intensity modulation transfer function of an optical system with PMD and PDL," IEEE Photon. Technol. Lett. **14**, 1515-1517, (2002).
32. S. Pitois, J. Fatome, and G. Millot, "Polarization attraction using counter-propagating waves in optical fiber at telecommunication wavelengths," Opt. Express **16**, 6646-6651, (2008).
33. A. Küng, L. Thévenaz, and P. A. Robert, "Polarization analysis of Brillouin scattering in a circularly birefringent fiber ring resonator," J. Lightwave. Technol. **15**, 977-982, (1997).
34. S. Randoux, and J. Zemmouri, "Polarization dynamics of a Brillouin fiber ring laser," Phys. Rev. A **59,** 1644-1653, (1999).
35. L. Thévenaz, S. Foaleng Mafang, and M. Nikles, "Fast measurement of local PMD with high spatial resolution using stimulated Brillouin scattering," paper 10.1.2 in *ECOC 2007*, Berlin, Germany, (2007).
36. X. Bao, J. Dhliwayo, N. Heron, D. J. Webb, and D. A. Jackson, "Experimental and theoretical studies on a distributed temperature sensor based on Brillouin scattering," J. Lightwave Technol. **13**, 1340-1348, (1995).
37. S. Chin, M. Gonzalez-Herraez, and L. Thévenaz, "Zero-gain slow and fast light propagation in an optical fiber," Opt. Express **14**, 10684-10692, (2006).
38. D. R. Walker, M. Bashkanski, A. Gulian, F. K. Fatemi, and M. Steiner, "Stabilizing slow light delay in stimulated Brillouin scattering using a Faraday rotator mirror," to be published on J. Opt. Soc. Am. B **25**, (2008).
39. A. Galtarossa, L. Palmieri, M. Santagiustina, L. Schenato, and L. Ursini, "Polarized Brillouin amplification in randomly birefringent and unidirectionally spun fibers," IEEE Photon Technol. Lett **20**, 1420-1422, (2008).

#102564 - $15.00 USD Received 9 Oct 2008; revised 18 Nov 2008; accepted 12 Dec 2008; published 16 Dec 2008

1. Introduction

Stimulated Brillouin Scattering (SBS) requires the lowest activation power of all non-linear effects in silica optical fibers. SBS has found numerous applications, including distributed sensing of temperature and strain [1-3], fiber lasers [4], optical processing of high frequency microwave signals [5-9], and even optical memories [10]. Over the last three years, SBS has been highlighted as the underlying mechanism in many demonstrations of variable group delay setups [11-16], often referred to as slow and fast light. In all of the above applications, SBS has been a favorable mechanism for its robustness, simplicity of implementation and low pump power in standard fibers at room temperature.

In SBS, a strong pump wave and a typically weak, counter-propagating signal wave optically *interfere* to generate, through electrostriction, a traveling longitudinal acoustic wave. The acoustic wave, in turn, couples these optical waves to each other [17,18]. The SBS interaction is efficient only when the difference between the optical frequencies of the pump and signal waves is very close (within a few tens of MHz) to a fiber-dependent parameter, the Brillouin shift ν_B, which is of the order of 10-11 GHz in silica fibers at room temperature and at telecommunication wavelengths [17,18]. An input signal whose frequency is ν_B lower than that of the pump (Stokes wave) experiences SBS amplification. If the input signal frequency is ν_B above that of the pump (anti-Stokes wave), SBS-induced signal attenuation is obtained instead. The strength of the interaction is often quantified in terms of an exponential gain coefficient γ, which is defined as the logarithm of the signal linear power gain (or loss), normalized to a unit pump power and unit fiber length $[\mathrm{W}\cdot\mathrm{m}]^{-1}$. (The coefficient γ equals the Brillouin gain factor g [19], divided by the fiber effective area).

Since SBS originates from optical interference between the pump and signal waves, the SBS interaction, at a given point along the fiber, is most efficient when the electric fields of the pump and signal are aligned, i.e., their vectors trace parallel ellipses and in the same sense of rotation. Conversely, if the two ellipses are again similar, but traced in opposite senses of rotation, with their long axes being orthogonal to each other, then the SBS interaction at that point averages to zero over an optical period. Consequently, in the presence of birefringence, the overall signal gain (or loss) depends on the birefringent properties of the fiber, as well as on the input states of polarization (SOPs) of both pump and signal. Following initial work by Horiguchi *et al*. [20], van Deventer and Boot [21] have studied in detail the signal SOPs leading to maximum and minimum gain. Based on the statistical properties of the evolution of the pump and signal SOPs in optical fibers much longer than the polarization beat length, but implicitly ignoring any influence of the Brillouin interaction on SOP evolution, they argued that for *standard*, low birefringence single-mode fibers, the maximum gain coefficient is twice that of the minimum one, and equals 2/3 of the maximum gain coefficient in a birefringence-free fiber γ_0. Furthermore, maximum gain is achieved when the pump and signal have identical polarizations (in their respective directions of propagation), while minimum gain is obtained for the corresponding 'orthogonal' case [21-24]. Their analysis was nicely corroborated by an experiment, which showed that for a given pump, there were indeed two input SOPs, chosen by the experimenters to be identical or orthogonal to that of the pump, with one providing an exponential gain twice that of the other one. However, the SBS amplification of an arbitrarily polarized input signal SOP was not discussed, nor was the role played by the Brillouin effect itself in the evolution of the signal SOP considered.

In this paper, the pioneering work of van Deventer and Boot is analytically substantiated and extended, using a vector formulation of the SBS amplification process in the presence of birefringence. A vector differential equation, combining both effects, is studied in the Jones and Stokes spaces. Based on the Jones space representation, it is shown that in the undepleted pump regime, the input signal SOPs which lead to maximum/minimum SBS gain are *always* orthogonal, regardless of pump power and the statistics of the pump and signal SOPs along the fiber. These maximum and minimum gain SOPs, therefore, provide a convenient vector

#102564 - $15.00 USD Received 9 Oct 2008; revised 18 Nov 2008; accepted 12 Dec 2008; published 16 Dec 2008

base for the examination of an arbitrarily polarized input signal wave. In the Stokes space, the evolution of the magnitude and the SOP of the signal wave along the fiber are described by a pair of coupled, rather simple differential equations. Using this representation, it is analytically shown that the SBS overall gain coefficient is determined by an average over a local mixing coefficient, similar (but not identical) to that of [21], for *any* input SOP, polarization statistics, or pump power. In addition, we show that in the presence of a pump, the evolution of the signal SOP is controlled not only by the fiber birefringence but also by the *local* SBS interaction, which drags the signal SOP towards that of the pump. The equations provide insight into the relation between the signal SOPs, which lead to maximum and minimum gain, and the SOP of the pump. The magnitude and SOP of the signal are then studied numerically. The maximum and minimum SBS gain coefficient for a general birefringent fiber are found to always be $\frac{1}{2}\gamma_0(1\pm\mu)$, $0\le\mu\le 1$. Even for a weakly birefringent fiber, μ does not necessarily need to be 1/3, although in the limit of a fiber embodying the fully developed statistics of [21], it tends to this value. The SOPs of input signals, which experience maximum/minimum gains, are then studied as a function of the pump power.

The signal SOP is also examined experimentally, for both Stokes and anti-Stokes signal waves. As predicted by the analysis, the output signal SOP is seen to converge towards a specific, preferred SOP, which is practically independent of both the input signal SOP and polarization transformations along the fiber [25]. That preferred output SOP could be arbitrarily varied, however, by changing the input pump SOP.

The remainder of this paper is organized as follows: Section 2 presents vector theoretical analysis of the signal wave, subject to both SBS and birefringence, in the undepleted pump regime. Section 3 is dedicated to numerical simulations. Section 4 provides experimental results, and brief concluding remarks are given in section 5.

2. Theory

Let us denote the column Jones vector of a monochromatic signal wave as $\vec{E}_{sig}(z)$, z indicating position along the fiber, with the launch and exit points at $z=0$ and $z=L$, respectively (L is the fiber length). With no pump, the propagation of $\vec{E}_{sig}(z)$ can be described by:

$$\vec{E}_{sig}(z)=\mathbf{T}(z)\vec{E}_{sig}(0) \tag{1}$$

with $\mathbf{T}(z)$ a unitary Jones matrix representing the effect of fiber birefringence. The pump wave, whose Jones vector is denoted by $\vec{E}_{pump}(z)$, is launched into the fiber at $z=L$. Throughout this paper, we work in the same right-handed coordinate system $\{x,y,z\}$, where the signal propagates in the positive z direction, while the pump propagates in the negative z direction. Thus, if both $\vec{E}_{sig}(z)$ and $\vec{E}_{pump}(z)$ equal the 2X1 vector $[1\ j]^T$ (T stand for transpose), they represent a right-handed circularly polarized signal and a left-handed circularly polarized pump wave, respectively [23,24]. We also neglect linear polarization-dependent power losses in the fiber, although such losses can be easily included in the analysis. Further, since the Brillouin shift ν_B is merely ~10GHz, and only a few kilometers of modern fibers are concerned, polarization mode dispersion can be ignored and, therefore, shifting the optical frequency by ν_B has a negligible effect on the Jones matrix of the fiber. Hence, the propagation of the pump wave (in the absence of a probe) can also be expressed using $\mathbf{T}(z)$:

$$\vec{E}_{pump}(0)=\mathbf{T}^T(z)\vec{E}_{pump}(z)\rightarrow\vec{E}_{pump}(z)=\mathbf{T}^*(z)\vec{E}_{pump}(0)\ ; \tag{2}$$

where $\mathrm{inv}[\mathbf{T}^T(z)]=\mathbf{T}^*(z)$.

#102564 - $15.00 USD Received 9 Oct 2008; revised 18 Nov 2008; accepted 12 Dec 2008; published 16 Dec 2008

When both the probe and pump waves are present, the *local* evolution of $\vec{E}_{sig}(z)$ and $\vec{E}_{pump}(z)$ is driven by both the fiber birefringence and the SBS effect to give (see [26] for the birefringence term, and [27] for the SBS term):

$$\frac{d\vec{E}_{sig}(z)}{dz} = \left[\frac{d\mathbf{T}(z)}{dz}\mathbf{T}^{\dagger}(z) + \frac{\gamma_0}{2}\left[\vec{E}_{pump}(z)\vec{E}^{\dagger}_{pump}(z)\right]\right]\vec{E}_{sig}(z) \tag{3a}$$

$$\frac{d\vec{E}_{pump}(z)}{dz} = \left[\frac{d\mathbf{T}^{*}(z)}{dz}\mathbf{T}^{T}(z) + \frac{\gamma_0}{2}\vec{E}_{sig}(z)\vec{E}^{\dagger}_{sig}(z)\right]\vec{E}_{pump}(z) \tag{3b}$$

γ_0 $[\mathrm{W\cdot m}]^{-1}$ is the SBS gain per unit length per a unit of pump power for a scalar interaction (i.e., for a fiber with no birefringence), and depends on the fiber material properties, the mode field diameter, the pump optical spectrum and the frequency offset between the pump and signal waves. We dedicate most of the analysis to the Stokes wave scenario, so that γ_0 is positive, but the analysis and results, properly interpreted, are equally valid for the anti-Stokes case, where the optical frequency of the signal is ν_B above that of the pump. The anti-Stokes signal surrenders its power to the pump, thereby becoming attenuated with an SBS attenuation per unit length of $-\gamma_0$. Note that $(\gamma_0/2)\left[\vec{E}_{pump}(z)\vec{E}^{\dagger}_{pump}(z)\right]$ is a 2×2 matrix, representing the outer product of a column vector ($\vec{E}_{pump}(z)$) with a row one (the transpose conjugate of $\vec{E}_{pump}(z)$).

From now on it will be assumed that SBS-induced signal amplification or attenuation negligbly affect the pump (i.e., the so-called undepleted pump approximation [21]). Thus, the SBS term in Eq. (3b) can be ignored and Eq. (3a) becomes linear in $\vec{E}_{sig}(z)$. Therefore,

$$\vec{E}_{sig}(L) = \mathbf{H}\cdot\vec{E}_{sig}(0), \tag{4}$$

where $\mathbf{H}$ is a 2×2 matrix, which depends on the fiber birefringence, the fiber length L, the pump power, and its SOP at $z = L$. The matrix $\mathbf{H}$ is generally non-unitary. Nevertheless, it can be processed using the singular value decomposition (SVD) technique:

$$\mathbf{H} = \mathbf{U}\cdot\mathbf{S}\cdot\mathbf{V}^{\dagger} = \mathbf{U}\cdot\begin{bmatrix} G_1 & 0 \\ 0 & G_2 \end{bmatrix}\cdot\mathbf{V}^{\dagger}, \tag{5}$$

where $\mathbf{U}$ and $\mathbf{V}$ are unitary matrices, G_1, G_2 are real and positive and satisfy $G_1 > G_2 > 1$ in the case of SBS amplification and $1 > G_1 > G_2$ in the case of SBS attenuation.

Using this decomposition two orthogonal input signal Jones vectors can be identified, which provide the maximum and minimum signal output powers, namely:

$$\vec{E}^{in\_\max}_{sig} = \left[\mathbf{V}^{\dagger}\right]^{-1}\begin{bmatrix}1\\0\end{bmatrix} = \mathbf{V}\begin{bmatrix}1\\0\end{bmatrix};\quad \vec{E}^{in\_\min}_{sig} = \mathbf{V}\begin{bmatrix}0\\1\end{bmatrix} \tag{6}$$

The corresponding *output* Jones vectors are given by:

$$\vec{E}^{out\_\max}_{sig} = \mathbf{U}\cdot\mathbf{S}\cdot\mathbf{V}^{\dagger}\cdot\mathbf{V}\begin{bmatrix}1\\0\end{bmatrix} = \mathbf{U}\cdot\mathbf{S}\begin{bmatrix}1\\0\end{bmatrix} = G_1\mathbf{U}\begin{bmatrix}1\\0\end{bmatrix} \tag{7}$$

$$\vec{E}^{out\_\min}_{sig} = \mathbf{U}\cdot\mathbf{S}\cdot\mathbf{V}^{\dagger}\cdot\mathbf{V}\begin{bmatrix}0\\1\end{bmatrix} = \mathbf{U}\cdot\mathbf{S}\begin{bmatrix}0\\1\end{bmatrix} = G_2\mathbf{U}\begin{bmatrix}0\\1\end{bmatrix}$$

#102564 - $15.00 USD Received 9 Oct 2008; revised 18 Nov 2008; accepted 12 Dec 2008; published 16 Dec 2008

and are, therefore, also orthogonal. It is thus convenient to represent an arbitrarily polarized input signal using the orthogonal base of $\vec{E}_{sig}^{in\_\max}$, $\vec{E}_{sig}^{in\_\min}$:

$$\vec{E}_{sig}^{in} = \alpha_0 \vec{E}_{sig}^{in\_\max} + \beta_0 \vec{E}_{sig}^{in\_\min} \tag{8}$$

Using Eqs. (7) and (8), the output signal Jones vector and the signal power are:

$$\begin{aligned} \vec{E}_{sig}^{out} &= \alpha_0 G_1 \mathbf{U}\begin{bmatrix}1\\0\end{bmatrix} + \beta_0 G_2 \mathbf{U}\begin{bmatrix}0\\1\end{bmatrix} \\ P_{sig}^{out} &= \left|\alpha_0\right|^2 G_1^2 + \left|\beta_0\right|^2 G_2^2 \end{aligned} \tag{9}$$

When $G_1 >> G_2$, Eq. (9) suggests that unless α_0 is negligible, an arbitrarily polarized input signal will be drawn towards the SOP of $\vec{E}_{sig}^{out\_\max}$. These predictions are supported by experiments, to be described in section 4.

Next, we try to relate $\vec{E}_{sig}^{in\_\max}$, $\vec{E}_{sig}^{in\_\min}$ to the SOP of the pump wave. To that end, we have transformed Eq. (3) to the Stokes space (see Appendix):

$$\frac{dS_{0\_sig}(z)}{dz} = \frac{\gamma_0 P_{pump}(z)}{2}\left(1 + \hat{s}_{pump}(z)\cdot\hat{s}_{sig}(z)\right)S_{0\_sig}(z) \tag{10a}$$

$$\begin{aligned} \frac{d\,\hat{s}_{sig}(z)}{dz} &= \vec{\beta}(z)\times\hat{s}_{sig}(z) + \frac{\gamma_0 P_{pump}(z)}{2}\hat{s}_{sig}(z)\times\left(\hat{s}_{pump}(z)\times\hat{s}_{sig}(z)\right) \\ &= \vec{\beta}(z)\times\hat{s}_{sig}(z) + \frac{\gamma_0 P_{pump}(z)}{2}\left[\hat{s}_{pump}(z) - \left(\hat{s}_{pump}(z)\cdot\hat{s}_{sig}(z)\right)\hat{s}_{sig}(z)\right] \end{aligned} \tag{10b}$$

Here S_{0_sig} is the signal power, $\hat{s}_{sig} = \left[s_{1,sig} \quad s_{2,sig} \quad s_{3,sig}\right]^T$ and similarly $\hat{s}_{pump}$ are 3X1 normalized Stokes vectors $\left(s_{1,sig,pump}^2 + s_{2,sig,pump}^2 + s_{3,sig,pump}^2 = 1\right)$, describing the evolution of the polarizations of the counter-propagating signal and pump waves, respectively, and finally, P_{pump} denotes the pump power, which for the undepleted, lossless case is *z*-independent. The three-dimensional vector $\vec{\beta}(z)$ describes the fiber birefringence in Stokes space [26]:

$$\vec{\beta}\cdot\vec{\sigma} \equiv 2j\frac{d\mathbf{T}}{dz}\mathbf{T}^{\dagger}, \tag{11}$$

where $\vec{\sigma}$ is a row vector of Pauli spin matrices [26] (see also in the Appendix). The vector $\vec{\beta}(z)$ is aligned with the Stokes space representation of the local slow axis of birefringence [26]. Note that we express both Stokes vectors in the same right handed coordinate system, in which the signal wave propagates in the positive z direction. Therefore, the Stokes vector $\hat{s} = \left[0 \quad 0 \quad 1\right]^T$ represents a right-handed circular polarization for the signal wave, but a left-handed circular polarization for the pump.

Eq. (10a) is easily cast into a form:

$$\frac{d\ln\left(S_{0\_sig}\right)}{dz} = \frac{\gamma_0 P_{pump}(z)}{2}\left(1 + \hat{s}_{pump}\cdot\hat{s}_{sig}\right). \tag{12}$$

In the undepleted pump regime, the solution is readily obtained:

#102564 - $15.00 USD Received 9 Oct 2008; revised 18 Nov 2008; accepted 12 Dec 2008; published 16 Dec 2008

$$S_{0\_sig}^{out} = S_{0\_sig}^{in} \exp\left[\frac{\gamma_0 P_{pump}}{2}\int_0^L \left(1+\hat{s}_{pump}\cdot\hat{s}_{sig}\right)dz'\right] = S_{0\_sig}^{in} \exp\left[\frac{\gamma_0 P_{pump}}{2} L\left(1+\left\langle \hat{s}_{pump}\cdot\hat{s}_{sig}\right\rangle_L\right)\right] \quad (13)$$

$\left\langle \hat{s}_{pump}\cdot\hat{s}_{sig}\right\rangle_L$ is the scalar product of the pump and signal Stokes vectors, averaged over the fiber length. Thus, for any input SOP one can define an effective SBS gain, given by:

$$\gamma = \frac{\gamma_0}{2}\left(1+\left\langle \hat{s}_{pump}\cdot\hat{s}_{sig}\right\rangle_L\right) \quad (14)$$

Obviously, γ depends on the signal input SOP, as well as on the pump SOP.

Equation (10b) specifies two driving forces that control the evolution of the SOP along the fiber. The first, $\vec{\beta}\times\hat{s}_{sig}$, describes the birefringence-induced evolution of the signal SOP [26]. The same term also governs the evolution of the pump SOP, albeit in the opposite direction. The second term, $(\gamma_0/2)P_{pump}\left[\hat{s}_{pump}-\left(\hat{s}_{pump}\cdot\hat{s}_{sig}\right)\hat{s}_{sig}\right]$, represents the effect of SBS amplification on the signal SOP. This second term has a very interesting physical interpretation on the Poincare sphere: it is a vector, orthogonal to $\hat{s}_{sig}$, and tangentially (on the sphere surface) pointing towards $\hat{s}_{pump}$. This term signifies a force pulling $\hat{s}_{sig}$ towards $\hat{s}_{pump}$. The magnitude of this pulling force scales with the pump power and depends on the local projection of $\hat{s}_{pump}(z)$ on $\hat{s}_{sig}(z)$, vanishing when either $\hat{s}_{sig}$ is parallel to $\hat{s}_{pump}$ (pump and signal SOPs aligned) or anti-parallel to it (in the Stokes space, namely: orthogonal in the Jones space).

Several special cases are of particular interest. Let us consider a fiber with no birefringence, so that the evolution of the signal SOP is governed by SBS alone. If the input signal SOP is aligned with that of the pump, $\left(\hat{s}_{pump}\cdot\hat{s}_{sig}^{in}=1\right)$, then it follows from Eq. (10b) that the $d\hat{s}_{sig}/dz=0$. The signal SOP, therefore, remains aligned with that of the pump throughout the fiber. Since in this case $\left\langle \hat{s}_{pump}\cdot\hat{s}_{sig}\right\rangle_L=1$, the SBS gain coefficient of Eq. (14) equals γ_0. Alternatively, when the signal input SOP is orthogonal to that of the pump $\left(\hat{s}_{pump}\cdot\hat{s}_{sig}^{in}=-1\right)$, we still obtain $d\hat{s}_{sig}/dz=0$, and the pump and signal remain orthogonal for all $0\le z\le L$. Now $\left\langle \hat{s}_{pump}\cdot\hat{s}_{sig}\right\rangle_L=-1$ and the SBS gain coefficient is zero. Thus, $\vec{E}_{sig}^{out\_\max}$ ($\vec{E}_{sig}^{out\_\min}$) in a birefringence-free fiber is parallel (perpendicular) to $\vec{E}_{pump}(z=L)$ (using our conventions, $\vec{E}_{sig}^{out\_\max}$ for a right-handed circularly polarized pump is left-handed polarized). When the input signal is arbitrarily polarized, the SBS polarization pulling term of Eq. (10b) is nonzero, so that $\hat{s}_{sig}$ is gradually drawn towards $\hat{s}_{pump}$. The slope of the gain coefficient versus pump power curve, determined by $\left\langle \hat{s}_{pump}\cdot\hat{s}_{sig}\right\rangle_L$, will increase with pump power (or fiber length), eventually approaching its maximum value of $\gamma_0 L$, and the SOP of the emerging signal will draw nearer and nearer that of the pump wave. These trends are, of course, fully consistent with the Jones space description of Eq. (9).

We now turn to the more prevalent scenario of standard single-mode fibers, where the birefringence term Eq. (10b) is larger than the SBS term (for a an average beat length of 40 m, $\left\langle\left|\vec{\beta}\right|\right\rangle_z \sim 0.16\ \mathrm{m}^{-1}$ whereas $\gamma_0 P_{pump}/2 \sim 0.01\mathrm{m}^{-1}$ for $\gamma_0 = 0.2\ [\mathrm{m}\cdot\mathrm{W}]^{-1}, P_{pump}=0.1\mathrm{W}$). While being relatively small, the SBS term cannot be ignored. High differential gains ($G_1/G_2 > 10$) are easily observed, and according to Eq. (9), any signal, whose input SOP even slightly

#102564 - $15.00 USD Received 9 Oct 2008; revised 18 Nov 2008; accepted 12 Dec 2008; published 16 Dec 2008

deviates from that of $\vec{E}_{sig}^{in\_\min}$, will emerge with its SOP being pulled towards that of $\vec{E}_{sig}^{out\_\max}$. While the polarization pulling is due to the SBS term, the final signal SOP is *not* that of $\vec{E}_{pump}(z=L)$. The relation between the SOP of $\vec{E}_{sig}^{out\_\max}$ and that of $\vec{E}_{pump}(z=L)$ are studied below, first analytically, in the low pump power limit, and then, numerically for the general case.

Let us assume first a very weak pump so that the Brillouin term in Eq. (10b) can be ignored ($G_1/G_2 \xrightarrow[P_{pump}\to 0]{} 1$). In this limit, the forward evolution of $\hat{s}_{sig}$ and the backward evolution of $\hat{s}_{pump}$ are *solely* governed by the birefringence term. We denote the maximum value of $\left\langle \hat{s}_{pump}\cdot\hat{s}_{sig}\right\rangle_L$ over all possible SOPs of the input signal $\hat{s}_{sig}(z=0)$, but for a given pump SOP ($\hat{s}_{pump}(z=L)$), as $\max_{\hat{s}_{sig}(z=0)}\left\{\left\langle \hat{s}_{pump}\cdot\hat{s}_{sig}\right\rangle_L\right\}$. But:

$$\begin{aligned}\left\langle \hat{s}_{pump}\cdot\hat{s}_{sig}\right\rangle_L \approx \left\langle \hat{s}_{pump}(z)\cdot\hat{s}_{sig}(z)\right\rangle_{\substack{Ensemble\\Average}} &= \left\langle \hat{s}_{pump}^T(0)\mathbf{M}_{\mathbf{T}^*}^T(z)\cdot\mathbf{M}_{\mathbf{T}}(z)\hat{s}_{sig}(0)\right\rangle_{\substack{Ensemble\\Average}}\\ &= \hat{s}_{pump}^T(0)\left\langle \mathbf{M}_{\mathbf{T}^*}^T\cdot\mathbf{M}_{\mathbf{T}}(z)\right\rangle_{\substack{Ensemble\\Average}}\hat{s}_{sig}(0)\\ &= \hat{s}_{pump}^T(0)\begin{bmatrix}\frac{1}{3} & & \\ & \frac{1}{3} & \\ & & -\frac{1}{3}\end{bmatrix}\hat{s}_{sig}(0).\end{aligned} \tag{15}$$

Here $\mathbf{M}_{\mathbf{T}}(z)$ and $\mathbf{M}_{\mathbf{T}^*}(z)$ are the Mueller matrices representing $\mathbf{T}(z)$ and $\mathbf{T}^*(z)$, respectively (T stands for transpose), and the fiber is assumed to be long enough so that most z values are much larger than many correlation lengths of the random birefringence. Finally, the ensemble averaged value of $\left\langle \mathbf{M}_{\mathbf{T}^*}^T(z)\cdot\mathbf{M}_{\mathbf{T}}(z)\right\rangle$ was taken from [28].

One can easily conclude from Eq. (15) that $\max_{\hat{s}_{sig}(z=0)}\left\{\left\langle \hat{s}_{pump}\cdot\hat{s}_{sig}\right\rangle_L\right\}$ is 1/3, resulting in a maximum achievable gain coefficient of $(2/3)\gamma_0$ (Eq. 14, see also a discussion in [21]). This maximum is attained when $\hat{s}_{sig}(z=0)$ is the image of $\hat{s}_{pump}(z=0)$ on the Poincare sphere, with the equatorial plane acting as a mirror, namely: $\hat{s}_{1,sig}^{\max}(0)=\hat{s}_{1,pump}(0)$, $\hat{s}_{2,sig}^{\max}(0)=\hat{s}_{2,pump}(0)$ and $\hat{s}_{3,sig}^{\max}(0)=-\hat{s}_{3,pump}(0)$. This $\hat{s}_{sig}^{\max}(z=0)$ is the normalized Stokes representation of the complex conjugate of the pump Jones vector at $z=0$, namely, $\vec{E}_{pump}^{*}(z=0)$, rather than that of $\vec{E}_{pump}(z=0)$ (as in the birefringence-free case). Conversely, $\min_{\hat{s}_{sig}(z=0)}\left\{\left\langle \hat{s}_{pump}\cdot\hat{s}_{sig}\right\rangle_L\right\}=-1/3$, corresponding to a minimum gain coefficient of $(1/3)\gamma_0$. This minimum value is attained for $\hat{s}_{sig}^{\min}(z=0)=-\hat{s}_{sig}^{\max}(z=0)$, which is the Stokes representation of a polarization orthogonal to that of $\vec{E}_{pump}^{*}(z=0)$, to be denoted by $\vec{E}_{pump}^{*\perp}(z=0)$. It is easily proven from Eqs. (1-2) that for a unitary $\mathbf{T}(z)$ (and ignoring the Brillouin term), if $\vec{E}_{sig}$ and $\vec{E}_{pump}^{*}$ are a parallel pair at $z=0$, they will continue to be parallel for all $0\le z\le L$, so that $\vec{E}_{sig}^{out\_\max}(z=L)$ has the same polarization as that of $\vec{E}_{pump}^{*}(z=L)$. These analytically obtained results are no different than the seemingly intuitively-drived conclusions of [21], when carefully noting the difference in the reference frame convention, but both approaches are strictly valid only in the limit of very weak pump power. The relation between $\vec{E}_{sig}^{\max}$ and $\vec{E}_{pump}^{*}$ in the presence of non-negligible level of pump power is investigated in the next section.

#102564 - $15.00 USD Received 9 Oct 2008; revised 18 Nov 2008; accepted 12 Dec 2008; published 16 Dec 2008

3. Simulations for Signal amplification (Stokes) and attenuation (anti-Stokes)

The SBS amplification/attenuation and the output SOP of the amplified/attenuated signal for different pump power levels were numerically examined, using Eqs. (2), (3) and (10a-10b). Simulations were based on the commonly used concatenated random wave-plate model [29], with the three components of $\vec{\beta}$ of Eq. (11) normally distributed with zero mean and the same standard deviation, chosen so that the average beat length $L_B \equiv 2\pi \Big/ \left\langle \left| \vec{\beta} \right| \right\rangle_z$ equals 40 m. Although a broad set of parameters was numerically investigated, results below were obtained for a fiber length L of 2250 m comprising 10,000 plates and $\gamma_0 = 0.2[\mathrm{W \cdot m}]^{-1}$.

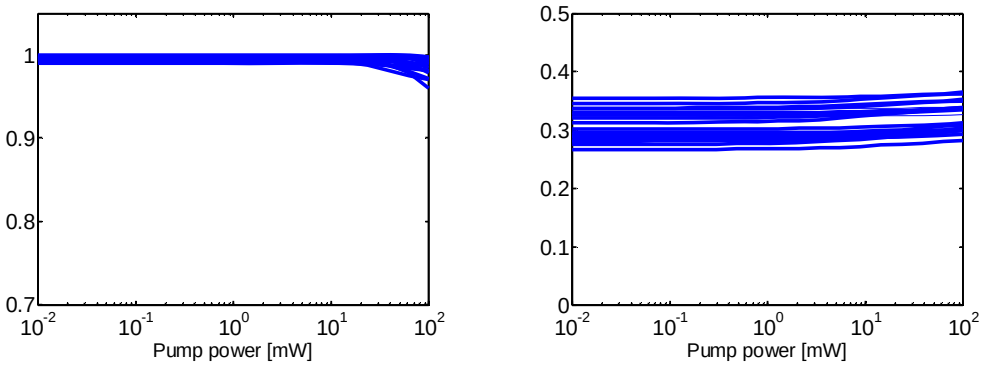

Fig. 1. (a). The projection, $\hat{s}_{sig}^{in\_\max} \cdot \hat{s}_{pump^*}(z=0)$, of the input signal (normalized) Stokes vector for maximum SBS gain, onto the (normalized) Stokes vector corresponding to $\vec{E}_{pump}^{\,*}(z=0)$, as a function of pump power, for 20 different fiber realizations. (b) The pump power dependence of $\max_{\hat{s}_{sig}(z=0)} \left\{ \left\langle \hat{s}_{pump} \cdot \hat{s}_{sig} \right\rangle_L \right\}$ for the same realizations. The beat length in all realizations was 40 m.

Figure 1(a) shows the projection of $\hat{s}_{sig}^{in\_\max}$ on $\hat{s}_{pump^*}(z=0)$, where $\hat{s}_{sig}^{in\_\max}$ and $\hat{s}_{pump^*}(0)$ are the normalized Stokes-space counterparts of $\vec{E}_{sig}^{\,in\_\max}$ and $\vec{E}_{pump}^{\,*}(z=0)$, respectively. Figure 1(b) shows the calculated $\left\langle \hat{s}_{pump} \cdot \hat{s}_{sig} \right\rangle_L$ for an input signal SOP aligned with $\vec{E}_{sig}^{\,in\_\max}$, as a function of pump power. The figures include several different fiber realizations, each with different random drawings of $\vec{\beta}$ values for the concatenated wave-plates, though all with an average beat length of 40 m. At low pump powers $\hat{s}_{sig}^{in\_\max} \cdot \hat{s}_{pump^*}(z=0)$ does not depend on P_{pump}, as discussed above, and the relatively small misalignments between $\vec{E}_{sig}^{\,in\_\max}$ and $\vec{E}_{pump}^{\,*}(0)$, as well as the deviations of $\left\langle \hat{s}_{pump} \cdot \hat{s}_{sig} \right\rangle_L$ from the predicted value of 1/3, are due to the finiteness and discreteness of the model. It is clearly seen that $\vec{E}_{sig}^{\,in\_\max}$ remains closely aligned with $\vec{E}_{pump}^{\,*}(z=0)$, even for a pump power as high as 100 mW. While not shown, this close alignment also holds at the fiber output, $z=L$, where the SOP of $\vec{E}_{sig}^{\,out\_\max}$ lies in a similar close vicinity that of $\vec{E}_{pump}^{\,*}(z=L)$.

Clearly, $\max_{\hat{s}_{sig}(z=0)} \left\{ \left\langle \hat{s}_{pump} \cdot \hat{s}_{sig} \right\rangle_L \right\}$, while not exactly 1/3 (Fig. 1(b)), depends very weakly on P_{pump}, resulting in a practically linear relationship between the achievable max/min gain coefficient and pump power. Figure 2 shows the signal power gain as a function of pump

#102564 - $15.00 USD Received 9 Oct 2008; revised 18 Nov 2008; accepted 12 Dec 2008; published 16 Dec 2008

power, for a signal SOP aligned with either $\vec{E}_{sig}^{\,in\_\max}$ (maximum gain), or $\vec{E}_{sig}^{\,in\_\min}$ (minimum gain). According to Eq. (14) and regardless of the particular fiber realization, the ratio of the slope of the maximum gain curve to that of the minimum gain at a particular P_{pump}, while not exactly 2, is always $\left(1+\max_{\hat{s}_{sig}(z=0)}\left\{\left\langle \hat{s}_{pump}\cdot\hat{s}_{sig}\right\rangle_L\right\}\right)\Big/\left(1-\max_{\hat{s}_{sig}(z=0)}\left\{\left\langle \hat{s}_{pump}\cdot\hat{s}_{sig}\right\rangle_L\right\}\right)$.

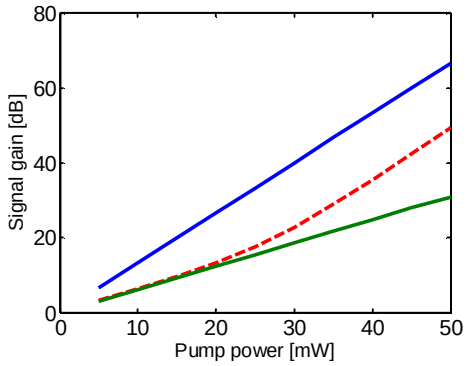

Fig. 2. Signal gain as a function of pump power for different SOPs of the input signal. The linear curves are calculated for an input SOP, aligned with either the pump-dependent $\vec{E}_{sig}^{\,in\_\max}$ (blue-top line), or orthogonal to it, i.e., parallel to $\vec{E}_{sig}^{\,in\_\min}$ (green-bottom line). The red-dashed line is for the case where the input SOP deviates from $\vec{E}_{sig}^{\,in\_\min}(P_{pump}=50\text{mW})$ by a $\pi/20$ rad rotation about the $\hat{s}_1$ axis on the Poincare sphere

Yet, SBS still has a dramatic effect on the output SOP of an input signal, whose SOP only slightly deviates from that of $\vec{E}_{sig}^{\,in\_\min}$, (see Fig. 2). As the difference between the minimum and maximum gains increases, the red-dashed gain curve in Fig. 2 changes its slope, approaching that of the maximum gain case. Incidentally [21], the same argument applies to amplified spontaneous SBS, which, therefore, under high differential gain conditions, emerges from the fiber with the SOP of $\vec{E}_{pump}^{\,*}(z=L)$. Thus, under high differential gain conditions the SOP of amplified spontaneous SBS at the fiber output ($z=L$) coincides with that of $\vec{E}_{sig}^{\,out\_\max}$!

For arbitrarily polarized input signals and for pump powers above 25 mW, the output signal SOPs are clearly seen in Fig. 3(a) and Fig. 3(b) to converge towards the SOP of $\vec{E}_{sig}^{\,out\_\max}$, which is almost unaffected by pump power. Figure 3(c) shows the evolution of $\hat{s}_{pump*}(z)\cdot\hat{s}_{sig}(z)$ as a function of the position coordinate z along the fiber, for different pump powers, when the signal input SOP is $\vec{E}_{pump}^{\,*\perp}(z=0)$. That input SOP is close to, but not quite equal to $\vec{E}_{sig}^{\,in\_\min}$, especially at high pump powers. Note the gradual pulling of signal SOP towards that of $\vec{E}_{pump}^{\,*}(z)$, requiring many beat lengths before the effect becomes quite distinct at high pump powers.

#102564 - $15.00 USD Received 9 Oct 2008; revised 18 Nov 2008; accepted 12 Dec 2008; published 16 Dec 2008

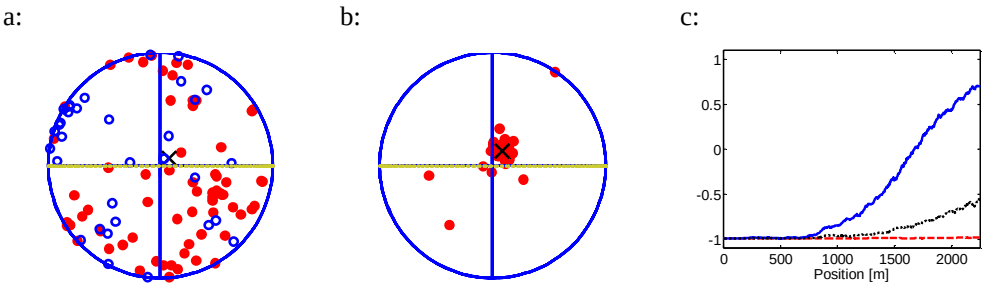

Fig. 3. (a) and (b): Scatter plots of output amplified signal SOP on the Poincare sphere, corresponding to 100 random input signal SOPs, for a specific fiber realization. The input pump Stokes vector $\hat{s}_{pump}$ was chosen as $[0 \quad 1 \quad 0]^T$. The horizontal and vertical axes in all figures correspond to the Stokes s_1 and s_3 axes, respectively. Red closed circles indicate SOPs for which s_2 is positive, whereas open blue squares indicate a negative s_2. 'X' denotes the location $\vec{E}_{sig}^{out\_max}$ in Stokes space. The pump power was 5 mW (a) and 50 mW (b). (c): Stokes space projection of the signal SOP on the conjugate of the pump SOP, $\hat{s}_{pump^*}(z) \cdot \hat{s}_{sig}(z)$, as a function of position for an input signal SOP exactly orthogonal to that of $\vec{E}^*_{pump}(z=0)$. Pump power was 25 mW (red dashed), 40 mW (black dotted) and 50 mW (blue solid).

The above analysis was provided for the Stokes wave. However, the anti-Stokes case can be treated very similarly. As in the Stokes wave scenario, the SBS interaction for an anti-Stokes signal is still maximum for an input SOP aligned with $\vec{E}^*_{pump}(0)$. However, this interaction results in efficient signal attenuation, rather than signal gain. We can, therefore, expect stronger attenuation for that input signal field component aligned with $\vec{E}^*_{pump}(0)$, and weaker attenuation ('maximum gain') for the orthogonal component. Correspondingly, the SOP of the emerging signal is dominated by that of the maximum power SOP, and is expected to be closely aligned with that of $\vec{E}^{*\perp}_{pump}(z=L)$. Figure 4 shows the scatter plots of the attenuated anti-Stokes signal, for $\hat{s}_{pump} = [0\ 1\ 0]^T$, indicating convergence towards $[0 -1\ 0]^T$, which is the (normalized) Stokes-spaced representation of $\vec{E}^{*\perp}_{pump}(z=L)$. Both scenarios are visited in the experiment, to be described next.

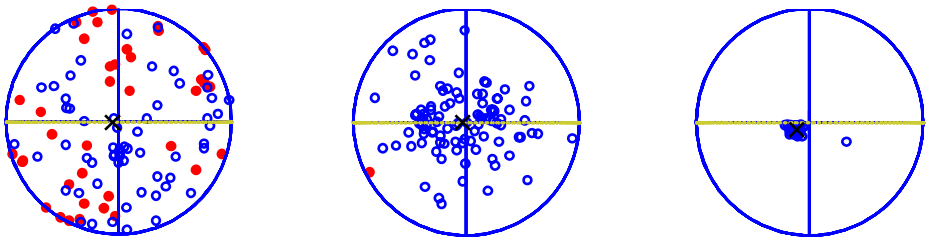

Fig. 4. Scatter plots of attenuated output signal SOP on the Poincare sphere, corresponding to 100 random input signal SOPs, for a specific fiber realization. The input pump Stokes vector $\hat{s}_{pump}$ was chosen as $[0 \quad 1 \quad 0]^T$. The horizontal and vertical axes in all figures correspond to Stokes s_1 and s_3 axes, respectively. Red closed circles indicate SOPs for which s_2 is positive, whereas open blue squares indicate a negative s_2. X' denotes the location $\vec{E}_{sig}^{out\_max}$ in Stokes space. The pump power was 5 mW (left), 25 mW (center) and 50 mW (right).

#102564 - $15.00 USD Received 9 Oct 2008; revised 18 Nov 2008; accepted 12 Dec 2008; published 16 Dec 2008

4. Experiment

The experimental setup for characterizing polarization related properties of SBS is shown in Fig. 5. Light emitted from a tunable laser source was split by a 50% coupler. In the lower (pump) branch, the light was amplified by a high-power Erbium-doped fiber amplifier (EDFA), and directed into the fiber under test via a circulator. The length of the fiber under test was 2250 m, and its Brillouin frequency shift was $\nu_B = 10.57\,\mathrm{GHz}$. The pump power was controlled by a variable optical attenuator (VOA). In the upper (signal) branch, the laser light was modulated by an electro-optic intensity modulator (EOM). The modulation frequency was tuned to ν_B, and the EOM bias voltage was adjusted to suppress the optical carrier [2]. Following the EOM, the signal was filtered by a narrow-band Fiber Bragg grating (FBG). For SBS signal amplification measurements, the frequency of the tunable laser was adjusted so that the lower modulation sideband matched the FBG reflection frequency [30]. This way, the frequency of the signal propagating in the fiber under test was ν_B below that of the pump. For SBS attenuation measurements, the tunable laser frequency was modified so that the upper modulation sideband was retained by the FBG [30]. Following the SBS interaction, the signal was routed to a power meter, followed by a lock-in amplifier to filter out spontaneous SBS, or to a polarization analyzer for the measurement of the signal output power and SOP. A second FBG in the detection path was used to filter out the backscattered pump, as well as the spontaneous Brillouin scattering amplified by the Stokes process in the SBS loss scenario.

For each pump power, the input signal SOPs which corresponded to minimum and maximum signal output power were found using the following procedure: First, a programmable polarization controller (Prog. PC) in the signal path was set to four non-degenerate SOPs, and the output signal power was recorded for each. Based on these four measurements, the top row of the 4X4 Mueller matrix describing the pumped fiber under test was extracted [31], and signal SOPs for minimum and maximum output power could be calculated. Next, the programmable PC was set to these two input SOPs and the output signal power was recorded.

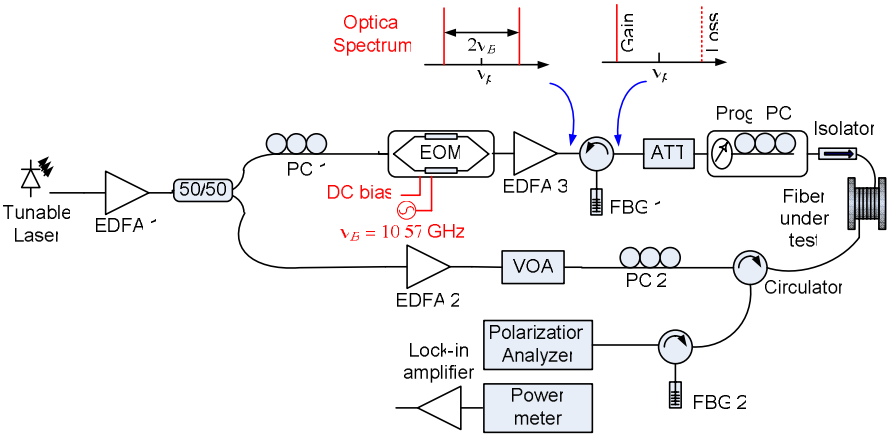

Fig. 5. Experimental setup for characterizing the polarization dependence of SBS. ATT: Optical attenuator. VOA: Variable optical attenuator. FBG: Fiber Bragg grating. DSB: Double side band modulation. SSB: single side band modulation. PC: Polarization controller. EDFA: Erbium-doped fiber amplifier. EOM: electro-optic modulator. ν_p denotes the optical frequency of the pump

Figure 6(a) shows the logarithm of the signal power gain (Stokes signal) as a function of pump power, for three different SOPs of the input signal wave. In the upper and lower curves, the signal SOP is adjusted for each pump power level to achieve maximum and minimum gain, respectively. In these curves, the logarithmic SBS gain appears to be linearly proportional to the pump power over the entire measurement range, indicating a power-

#102564 - $15.00 USD Received 9 Oct 2008; revised 18 Nov 2008; accepted 12 Dec 2008; published 16 Dec 2008

independent gain coefficient, as obtained in simulations. Furthermore, the slope of the maximum gain curve is extremely close to twice that of the minimum gain curve [21]. These results indicate that our 2.2km fiber comprises many correlation lengths of the random birefringence [21, 28]. The third curve of Fig. 6(a) shows the logarithm of the SBS gain for a signal, whose input SOP, $\vec{E}_{sig(Stokes)}^{in\_near\_min}$, is azimuthally 40^0 away from $\vec{E}_{sig(Stokes)}^{in\_min}$. Initially, for relatively low pump power, the gain slope is that of the minimum gain curve. However, for higher pump powers, the measured gain increases rapidly and its slope approaches that of the maximum gain curve, as discussed in Sec. 3.

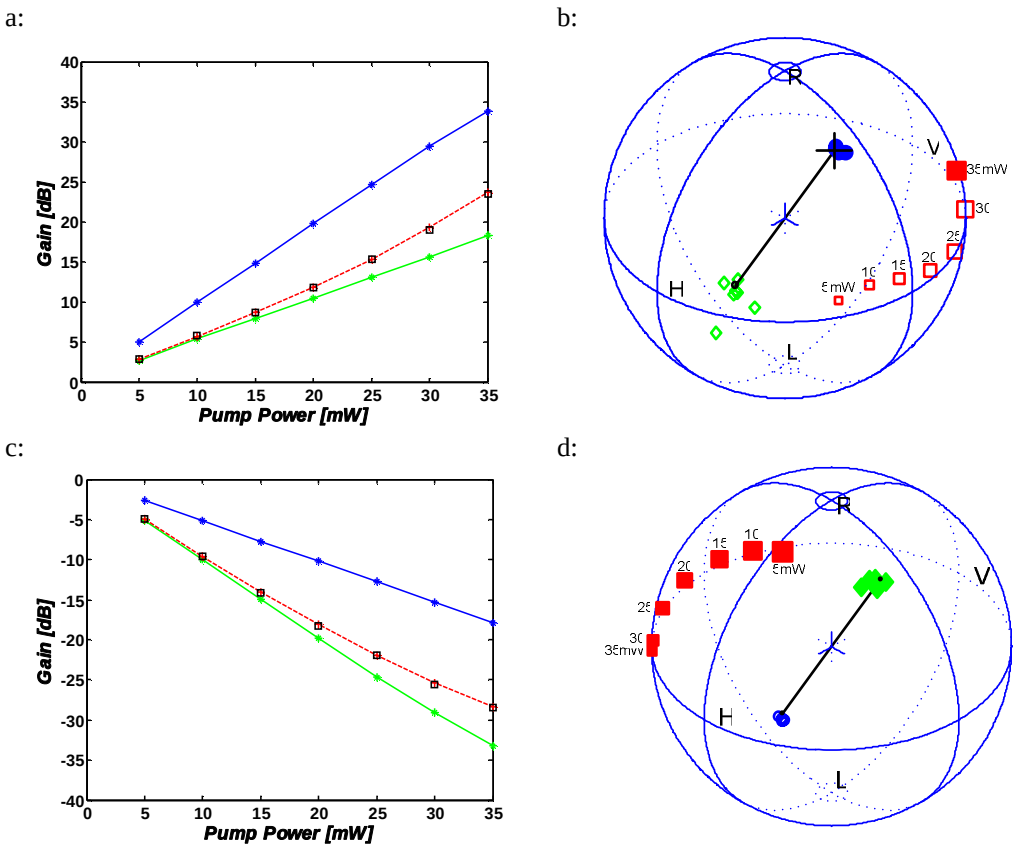

Fig. 6. (a). SBS gain (Stokes signal) in dB as a function of pump power, for a 2250 m long fiber. Lower curve (Green) – optimized for minimum gain, Upper curve (Blue) – optimized for maximum gain, Dashed curve (Red) – for an input SOP in the vicinity of $\vec{E}_{sig(Stokes)}^{in\_min}$, rotated from it by 40^0 around the s_3 (RL) axis (the black squares are explained in the text). (b) The SOPs of the emerging amplified signals for the three cases of (a): maximum (blue solid circles), minimum (green open diamonds), and red squares for the intermediate case. Open symbols denote SOPs in the back of the sphere. The size of the square is a measure of the signal power, *increasing* with pump power for Stokes signals. The black '+' is the SOP of the spontaneous SBS. The straight line through the center of the sphere connects this SOP to its orthogonal counterpart. (c) SBS attenuation (anti-Stokes signal) in dB as a function of pump power. Lower curve (Green) – optimized for minimum output power (maximum attenuation), Upper curve (Blue)– optimized for maximum output power (minimum attenuation), Dashed curve (Red) – for an input SOP in the vicinity of $\vec{E}_{sig(A-Stokes)}^{in\_min}$, rotated from it by 40^0 around the s_3 (RL) axis. (d) The SOPs of the emerging attenuated signals for the cases of (c): maximum (blue open circles), minimum (green solid diamonds), and red squares for the intermediate case. The straight line through the center of the sphere is that of (b), shown here for reference.

#102564 - $15.00 USD Received 9 Oct 2008; revised 18 Nov 2008; accepted 12 Dec 2008; published 16 Dec 2008

As a consistency check, we used Eqs. (8)-(9) first to project $\vec{E}_{sig(Stokes)}^{in\_near\_min}$ on the measured $\vec{E}_{sig(Stokes))}^{in\_max}$, $\vec{E}_{sig(Stokes)}^{in\_min}$, and then used the measured values for G_1 (maximum gain) and G_2 (minimum gain) to analytically predict the gain experienced by $\vec{E}_{sig(Stokes))}^{in\_near\_min}$. The results are shown as open squares on the dashed (red) curve in Fig. 6(a), demonstrating excellent agreement with the measured gain. Figure 6(b) shows the output SOPs corresponding to $\vec{E}_{sig(Stokes)}^{out\_max}$, $\vec{E}_{sig(Stokes)}^{out\_min}$ and $\vec{E}_{sig(Stokes)}^{out\_near\_min}$ for all pump powers. Also shown on the sphere is the SOP of spontaneously amplified Brillouin scattering, which was obtained by turning off the signal input and measuring the SOP of the Brillouin-scattered light at $\nu_s = \nu_p - \nu_B$. Note that as P_{pump} spans the 5-35mW range, $\left\{\vec{E}_{sig(Stokes)}^{out\_max}\right\}$ and $\left\{\vec{E}_{sig(Stokes)}^{out\_min}\right\}$ hardly change and they are fairly orthogonal to one another (the SOP readings of the polarization analyzer in the minimum gain case were contaminated by the spontaneously amplified Brillouin scattering, leading to a larger spread near $\left\{\vec{E}_{sig(Stokes)}^{out\_min}\right\}$). Furthermore, $\left\{\vec{E}_{sig(Stokes)}^{out\_max}\right\}$ coincides, as expected, with the SOP of the spontaneously amplified Brillouin scattering. Also shown is the evolution of the signal SOP for $\vec{E}_{sig(Stokes)}^{in\_near\_min}$, clearly indicating the pulling of its SOP towards that of $\left\{\vec{E}_{sig(Stokes)}^{out\_max}\right\}$. Figure 6(c) shows the logarithm of the maximum and minimum attenuation of an anti-Stokes signal. As obtained for the Stokes wave, the curves for maximum and minimum are linear, and the ratio of their slopes is close to two. Note that the obtained curves replicate those of the corresponding Stokes signal, albeit with a minus sign. The figure also shows the measured and calculated logarithmic loss of an anti-Stokes signal with an input SOP $\vec{E}_{sig(A-stokes)}^{in\_near\_min}$. Finally, Fig. 6(d) shows the output SOPs corresponding to $\vec{E}_{sig(A-Stokes)}^{out\_max}$, $\vec{E}_{sig(A-Stokes)}^{out\_min}$ and $\vec{E}_{sig(A-Stokes)}^{out\_near\_min}$ for all pump powers. Polarization pulling towards the SOP of $\left\{\vec{E}_{sig(A-Stokes)}^{out\_max}\right\}$ is observed. It is seen that $\left\{\vec{E}_{sig(A-Stokes)}^{out\_min}\right\}$ (solid diamonds in Fig. 6(d)), which suffers maximum attenuation are parallel to $\left\{\vec{E}_{sig(Stokes)}^{out\_max}\right\}$ (solid circles in Fig. 6(b)), which enjoys the maximum possible gain.

Figure 7 shows the signal output SOP for twenty different input SOPs, which were evenly distributed on the Poincare sphere. As the pump power is increased, the output signal SOPs converge to a particular, preferred state. Thus, the converging effect is effective for both SBS signal gain and signal loss, in the undepleted pump regime.

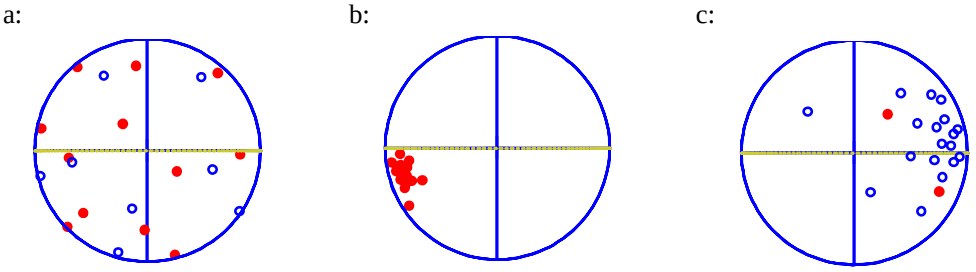

Fig. 7. Measured output signal SOP for SBS signal gain and SBS signal loss for twenty evenly distributed input signal SOPs. (a) Stokes SOP, pump power is 5 mW. (b) Stokes SOP, pump power is 45 mW. (c) Anti-Stokes SOP, pump power is 20mW (SOP measurements in the signal attenuation scenario were difficult due to the presence of spontaneous SBS, which competed with the attenuated signal. Thus, reliable readings could not be obtained for pump powers above 25 mW.)

#102564 - $15.00 USD Received 9 Oct 2008; revised 18 Nov 2008; accepted 12 Dec 2008; published 16 Dec 2008

5. Conclusions

In this work, the analysis of SBS in birefringent fibers was extended to include arbitrarily polarized signals. A vector propagation equation for the signal wave in the undepleted pump regime was provided, both in Jones and in Stokes spaces. The equations and their subsequent analysis provide expressions for the output signal vector, regardless of the polarization statistics of the pump and signal waves along the fiber. The analysis showed that SBS in the undepleted pump regime may be modeled as a pseudo-linear partial polarizer, whose input states for maximum and minimum gain are orthogonal. Due to the large difference in gain between these maximum and minimum states, it is expected that the SOP of an arbitrarily polarized input signal will be closely aligned with that of the maximum gain axis at the fiber output. This prediction was experimentally confirmed, for both Stokes and anti-Stokes signal waves. Somewhat similar polarization attraction between counter propagating waves, based on the Kerr effect in short, highly non-linear fibers, was recently reported [32], but the effect was restricted to circular SOPs. The vector properties of SBS can give rise to an arbitrary polarization synthesis. The analysis also shows that the maximum and minimum input signal SOPs for the Stokes wave in long, standard single-mode fibers correspond to the conjugate of the outgoing pump, and the orthogonal of that conjugate, respectively. This correspondence is practically valid for pump powers up to tens of milliwatts over fibers a few km long. The roles of the two SOPs are reversed for the anti-Stokes wave.

The polarization and birefringence dependence of SBS has already been used in Brillouin fiber lasers [33,34] and distributed birefringence measurements [35]. On the other hand, the same dependence can hinder the performance of distributed strain and temperature sensors [36], and SBS based slow light setups. In addition, birefringence was observed to cause a nonlinear response in the delay-pump power transfer function [37]. In one recent example, the polarization sensitivity of SBS-induced delay was overcome using a Faraday rotator mirror [38]. Clearly, the polarization related properties of SBS in long, standard single-mode fibers continue to be of large interest. The tools developed in this work provide a broad and comprehensive framework for the study of SBS and polarization and open new horizons for applications. A possible application, in which the spread of the signal output SOP for random input polarization serves as a measure of the fiber beat length, is currently under study.

Appendix

In this appendix, the Stokes space representation of the signal propagation equation in the presence of SBS and birefringence, Eq. (10a-10b), is derived (see [39] for a different, though equivalent, formulation, of the equations governing the evolution of the non-normalized signal Stokes vector). The starting point for the derivation is Eq. (3) repeated here for convenience:

$$\frac{d\vec{E}_{sig}(z)}{dz}=\left[\frac{d\mathbf{T}(z)}{dz}\mathbf{T}^{\dagger}(z)+\frac{\gamma_0}{2}\vec{E}_{pump}(z)\vec{E}^{\dagger}_{pump}(z)\right]\vec{E}_{sig}(z) \tag{A1}$$

$$\frac{d\vec{E}_{pump}(z)}{dz}=\left[\frac{d\mathbf{T}^{*}(z)}{dz}\mathbf{T}^{T}(z)+\frac{\gamma_0}{2}\vec{E}_{sig}(z)\vec{E}^{\dagger}_{sig}(z)\right]\vec{E}_{pump}(z) \tag{A2}$$

To obtain the evolution of the signal power and its SOP in terms of the Stokes parameters we use the common definitions [26, Eqs. (2.6), (3.5)] ($\vec{\sigma}$ is a vector of the Pauli spin matrices):

$$S^0\equiv\vec{E}^{\dagger}\vec{E}\;;\;\; S^0\hat{s}\equiv\vec{E}^{\dagger}\vec{\sigma}\vec{E}\;;\;\; \sigma_1=\begin{bmatrix}1 & 0\\ 0 & -1\end{bmatrix}\;,\;\; \sigma_2=\begin{bmatrix}0 & 1\\ 1 & 0\end{bmatrix}\;\text{and}\;\; \sigma_3=\begin{bmatrix}0 & -j\\ j & 0\end{bmatrix} \tag{A3}$$

and S^0 and $\hat{s}$ denote, respectively, the power and normalized Stokes vector which correspond to $\vec{E}$. Using Eq. (11) which reads:

#102564 - $15.00 USD Received 9 Oct 2008; revised 18 Nov 2008; accepted 12 Dec 2008; published 16 Dec 2008

$$\vec{\beta}\cdot\vec{\sigma} \equiv 2j\frac{d\mathbf{T}}{dz}\mathbf{T}^{\dagger}, \tag{A4}$$

and using the expansion of the projection operator in terms of Pauli matrices [26]:

$$\vec{E}\vec{E}^{\dagger} \equiv \frac{S_0}{2}\left(\mathbf{I} + \hat{s}\cdot\vec{\sigma}\right), \tag{A5}$$

with $\mathbf{I}$ denoting the 2X2 identity matrix, we obtain:

$$\frac{d\vec{E}_{sig}}{dz} = \left[-\frac{j}{2}\vec{\beta}\cdot\vec{\sigma} + \frac{\gamma_0 S^0_{pump}}{4}\left(\mathbf{I} + \hat{s}_{pump}\cdot\vec{\sigma}\right)\right]\vec{E}_{sig}\ . \tag{A6}$$

Eq. (A6) can be used to obtain an equation for the evolution of the signal power:

$$\frac{dS^0_{sig}}{dz} = \frac{d\left(\vec{E}^{\dagger}_{sig}\vec{E}_{sig}\right)}{dz} = \vec{E}^{\dagger}_{sig}\left[-\frac{j}{2}\vec{\beta}\cdot\vec{\sigma} + \frac{\gamma_0 S^0_{pump}}{4}\left(\mathbf{I} + \hat{s}_{pump}\cdot\vec{\sigma}\right)\right]\vec{E}_{sig} + \vec{E}^{\dagger}_{sig}\left[\frac{j}{2}\vec{\beta}\cdot\vec{\sigma} + \frac{\gamma_0 S^0_{pump}}{4}\left(\mathbf{I} + \hat{s}_{pump}\cdot\vec{\sigma}\right)\right]\vec{E}_{sig} = \frac{\gamma_0}{2}\left(1 + \hat{s}_{pump}\cdot\hat{s}_{sig}\right)S^0_{pump}\,S^0_{sig} \tag{A7}$$

The equation governing the propagation of the normalized signal Stokes vector can be derived using Eqs. (A.3)-(A7) of [26]:

$$\begin{aligned}
\frac{d\,\hat{s}_{sig}}{dz} &= \frac{d}{dz}\left(\frac{\vec{E}^{\dagger}_{sig}\vec{\sigma}\vec{E}_{sig}}{\vec{E}^{\dagger}_{sig}\vec{E}_{sig}}\right) = \frac{\left(\vec{E}^{\dagger}_{sig}\vec{E}_{sig}\right)d\left(\vec{E}^{\dagger}_{sig}\vec{\sigma}\vec{E}_{sig}\right)/dz - \left(\vec{E}^{\dagger}_{sig}\vec{\sigma}\vec{E}_{sig}\right)d\left(\vec{E}^{\dagger}_{sig}\vec{E}_{sig}\right)/dz}{\left(\vec{E}^{\dagger}_{sig}\vec{E}_{sig}\right)^2} \\
&= \left[d\left(\vec{E}^{\dagger}_{sig}\vec{\sigma}\vec{E}_{sig}\right)/dz - S^0_{sig}\hat{s}_{sig}\frac{\gamma_0 S^0_{pump}}{2}\left(1 + \hat{s}_{pump}\cdot\hat{s}_{sig}\right)\right]\Big/S^0_{sig} \\
&= \frac{1}{S^0_{sig}}\left[\left(\frac{d}{dz}\vec{E}^{\dagger}_{sig}\right)\vec{\sigma}\vec{E}_{sig} + \vec{E}^{\dagger}_{sig}\vec{\sigma}\left(\frac{d}{dz}\vec{E}_{sig}\right)\right] - \frac{\gamma_0 S^0_{pump}}{2}\left(1 + \hat{s}_{pump}\cdot\hat{s}_{sig}\right)\hat{s}_{sig} \\
&= \vec{\beta}\times\hat{s}_{sig} + \frac{\gamma_0 S^0_{pump}}{2}\left[\hat{s}_{sig} + \hat{s}_{pump}\right] - \frac{\gamma_0 S^0_{pump}}{2}\left(1 + \hat{s}_{pump}\cdot\hat{s}_{sig}\right)\hat{s}_{sig} \\
&= \vec{\beta}\times\hat{s}_{sig} + \frac{\gamma_0 S^0_{pump}}{2}\hat{s}_{pump} - \frac{\gamma_0 S^0_{pump}}{2}\left(\hat{s}_{pump}\cdot\hat{s}_{sig}\right)\hat{s}_{sig} = \vec{\beta}\times\hat{s}_{sig} + \frac{\gamma_0 S^0_{pump}}{2}\hat{s}_{sig}\times\left(\hat{s}_{pump}\times\hat{s}_{sig}\right)
\end{aligned} \tag{A8}$$

Following similar steps the corresponding equations for the pump can be derived. The resulting set of coupled equations is (with $\tilde{\vec{\beta}}$ defined by $\tilde{\beta}_1 = -\beta_1; \tilde{\beta}_2 = -\beta_2\ \tilde{\beta}_3 = +\beta_3$):

$$\begin{aligned}
&\frac{dS^0_{sig}}{dz} = \frac{\gamma_0}{2}\left(1 + \hat{s}_{pump}\cdot\hat{s}_{sig}\right)S^0_{pump}\,S^0_{sig} \qquad ; \qquad \frac{dS^0_{pump}}{dz} = \frac{\gamma_0}{2}\left(1 + \hat{s}_{sig}\cdot\hat{s}_{pump}\right)S^0_{sig}\,S^0_{pump} \\
&\frac{d\,\hat{s}_{sig}}{dz} = \vec{\beta}\times\hat{s}_{sig} + \frac{\gamma_0 S^0_{pump}}{2}\hat{s}_{sig}\times\left(\hat{s}_{pump}\times\hat{s}_{sig}\right) \qquad\qquad \frac{d\,\hat{s}_{pump}}{dz} = \tilde{\vec{\beta}}\times\hat{s}_{pump} + \frac{\gamma_0 S^0_{sig}}{2}\hat{s}_{pump}\times\left(\hat{s}_{sig}\times\hat{s}_{pump}\right)
\end{aligned} \tag{A9}$$

Acknowledgments

This work has been carried out within the framework of the European COST Action 299 – FIDES. M. Tur, E. Zilka and A. Eyal also wish to acknowledge the support of the Israeli Science Foundation (ISF). A. Zadok acknowledges the support of a doctoral research fellowship from the Clore Foundation, Israel, a post-doctoral research fellowship from the Center of Physics in Information (CPI), Caltech, and the Rothschild post-doctoral fellowship from Yad-Hanadiv Foundation, Israel.